

Article

The Effect of Obliquely Sputtered Cu Underlayers with Different Thicknesses on the Magnetic Properties of 50 nm Ni₈₀Fe₂₀ Thin Films

 Xiaoyu Li ^{1,2,3,*}, Yunshi Jiang ¹, Huan Yan ¹, Tianming Li ², Lu Zhang ¹, Zhihong Zhang ¹, Xian Guan ³, Min Chen ¹, Jiaoyin Wang ², Yihan Pu ¹, Genzhai Peng ¹ and Mengjia Wang ¹
¹ The Ninth Research Institute of China Electronics Technology Group, Mianyang 621000, China

² High-Power Radiation Laboratory, School of Electronic Science and engineering, University of Electronic Science and Technology of China, Chengdu 610051, China

³ Mianyang West Magnetic Technology Co, Ltd., Mianyang 621000, China

* Correspondence: lxyhope@126.com; Tel.: +86-177-0805-3791

Abstract: The magnetic properties of 50 nm Ni₈₀Fe₂₀ deposited on Cu underlayers with different thicknesses by obliquely sputtering were studied. It was found that the in-plane uniaxial magnetic anisotropy (IPUMA) of the Ni₈₀Fe₂₀ film can be induced by the obliquely sputtered Cu underlayer deposited under the NiFe layer. The IPUMA field of NiFe film varies between 20 Oe and 40 Oe when the thickness of Cu underlayer varies from 5 nm to 50 nm. The permeability spectrum results show that the damping factor increases with increasing Cu underlayer thickness. This indicates that changing the thickness of the Cu underlayer of obliquely sputtering is an effective method to adjust the damping factor in the dynamic magnetization process of Ni₈₀Fe₂₀ thin films.

Keywords: obliquely sputtered Cu underlayer; Ni₈₀Fe₂₀ films; dynamic magnetic properties; damping factor



Citation: Li, X.; Jiang, Y.; Yan, H.; Li, T.; Zhang, L.; Zhang, Z.; Guan, X.; Chen, M.; Wang, J.; Pu, Y.; et al. The Effect of Obliquely Sputtered Cu Underlayers with Different Thicknesses on the Magnetic Properties of 50 nm Ni₈₀Fe₂₀ Thin Films. *Magnetochemistry* **2022**, *8*, 134. <https://doi.org/10.3390/magnetochemistry8100134>

Academic Editor: Greg A. Brewer

Received: 22 August 2022

Accepted: 12 October 2022

Published: 19 October 2022

Publisher's Note: MDPI stays neutral with regard to jurisdictional claims in published maps and institutional affiliations.



Copyright: © 2022 by the authors. Licensee MDPI, Basel, Switzerland. This article is an open access article distributed under the terms and conditions of the Creative Commons Attribution (CC BY) license (<https://creativecommons.org/licenses/by/4.0/>).

1. Introduction

It is well known that the dynamic magnetization properties of soft magnetic films applied to high frequencies, the dynamic magnetization process can be represented by phenomenological LLG Equation (1) [1]:

$$\frac{d\vec{M}}{dt} = -\gamma(\vec{M} \times H_k) + \frac{\alpha}{4\pi M_s}(\vec{M} \times \frac{d\vec{M}}{dt}) \quad (1)$$

where M is the magnetic moment, $4\pi M_s$ is the saturation magnetization, H_k is the effective IPUMA field, α is the damping factor, and γ is the gyromagnetic ratio. The relationship between permeability and frequency of soft magnetic film materials with IPUMA can be obtained from LLG Equation (2) [2,3]. Its expression is as follows:

$$\mu = 1 + \frac{f_1(f_0 + f_1 + i\alpha_{eff}f)}{f_r^2 - f^2 + i f \Delta f_r} \quad (2)$$

where $f_1 = \gamma 4\pi M_s / 2\pi$, $f_0 = \gamma H_k / 2\pi$, $f_r^2 = f_0^2 + f_1 f_0$, and $\Delta f_r = \alpha(2f_0 + f_1)$. Both H_k and α are quite critical for soft magnetic films used in high frequency application.

The IPUMA field is a very important parameter, which determines the upper limit of high-frequency applications of soft magnetic devices [4,5]. Hence, understanding and adjusting the IPUMA field H_a of soft magnetic thin films has received great attention; however, effective adjusting of the damping factor α , which represents the rate of the magnetization reaching equilibrium position without external stimulus, has been rarely studied. Therefore, it also becomes particularly important to adjust the damping factor.

It has been reported that the anisotropic surface roughness of obliquely deposited Ta, Pt, Co, or Ru underlayers can induce high IPUMA [6–10]. When a ferromagnetic thin film is deposited at normal incidence, IPUMA is generated by the magnetostatic coupling caused by anisotropic fluctuations at the interface between the underlayer and the ferromagnetic layer. However, the thicknesses of the ferromagnetic layer are only a few nanometers ($0 \text{ nm} < t < 10 \text{ nm}$) corresponding to so-called ultrathin films in these experiments [6–10]. There are no relevant studies for a thicker ferromagnetic layer ($t \geq 50 \text{ nm}$) with an obliquely sputtered underlayer. Meanwhile, as previously reported, doping [11], exchange-coupling interactions [12], deposition of Cu cap layer on granular films [2], and changing sputtering conditions [13] all can be used to adjust the damping factor α effectively. But the influence of obliquely sputtered underlayer on the damping factor α in a continuous film has been seldom discussed.

Hence, in this work, we chose 50 nm $\text{Ni}_{80}\text{Fe}_{20}$ thin film as a ferromagnetic layer and a series of obliquely sputtered Cu layers with varying thickness t were used as underlayer. The effects of obliquely sputtered deposition of Cu underlayer of different thicknesses on the magnetic properties of 50 nm $\text{Ni}_{80}\text{Fe}_{20}$ films were investigated. We found that IPUMA can be obtained in all samples and the damping factor α has a significant correlation with the thickness of Cu underlayer.

2. Experimental

A series of $\text{Cu}(t)/\text{Ni}_{80}\text{Fe}_{20}$ samples were prepared on Si(111) substrates by RF magnetron sputtering at room temperature. The background pressure of the sputtering chamber is about $3 \times 10^{-5} \text{ Pa}$. During the deposition of the Cu underlayer, the Ar pressure and sputtering power were 0.4 Pa and 100 W, respectively. The sample deposition process is as follows: First, the Cu underlayer is prepared by obliquely sputtering. The sample holder is fixed during the preparation of the Cu layer to complete inclined sputtering [14]. After depositing Cu layer, 50 nm $\text{Ni}_{80}\text{Fe}_{20}$ thin films were deposited with 99.99% pure $\text{Ni}_{80}\text{Fe}_{20}$ target. During the deposition of $\text{Ni}_{80}\text{Fe}_{20}$ thin films, the sample holder was rotated at an angular velocity of 1.7 rads⁻¹ to obtain uniform film thickness, and the sputtering pressure and power were 0.4 Pa and 140 W, respectively. The film thickness is calculated based on the rate of deposition. Figure 1 is a schematic diagram of obliquely sputtering. We found that the direction of the easy magnetization axis (EA) is perpendicular to the deposition direction, while the hard magnetization axis (HA) is oriented along the deposition direction.

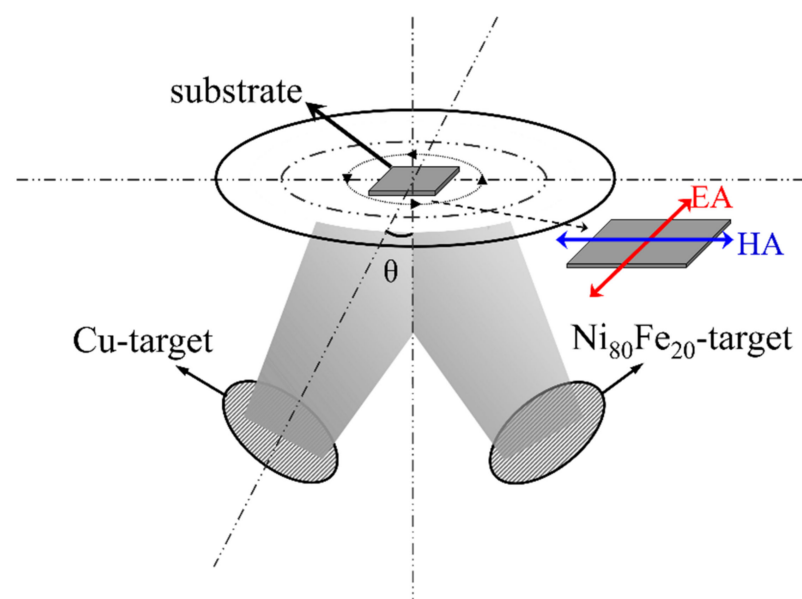


Figure 1. The schematic diagram of obliquely sputtering.

The thickness of the samples was measured using a surface profilometer (VEECO Dektak8 ADP-8) and the deposition rate was calculated. The surface morphology of the films was measured via field emission scanning electron microscopy (SEM, Hitachi S-4800). The dynamic magnetic properties of the samples were obtained by measuring the permeability spectra of the samples using a single-ended unbanded transmission line method [15], in the frequency range from 100 MHz to 5 GHz. The hysteresis loops of all samples were measured using a vibrating sample magnetometer (VSM). All the above measurements were performed at room temperature.

3. Results and Discussion

The static magnetic properties of the samples were obtained by measuring the in-plane hysteresis loops of the as-deposited Si/Cu (t nm)/Ni₈₀Fe₂₀ (50 nm) bilayer films. Figure 2a shows the M/M_s - H curves along the easy and hard axes of bilayer thin film samples with thicknesses increasing from 5 nm to 50 nm. It is found that the direction of the easy-axis of magnetization is perpendicular to the incident direction of the sputtered Cu particles. The remanence ratio of the easy-axis hysteresis loop is close to 1, showing a good squareness ratio, while the resigantion loop of the hard-axis hysteresis shows good linearity with extremely low remanence and low coercivity. This indicates that the obliquely sputtered Cu underlayer can induce a very pronounced IPUMA. Figure 2b,c are SEM photos of $t = 5$ nm and $t = 50$ nm thin film samples, respectively. It can be found that the particle size on the surface of $t = 50$ nm sample is larger.

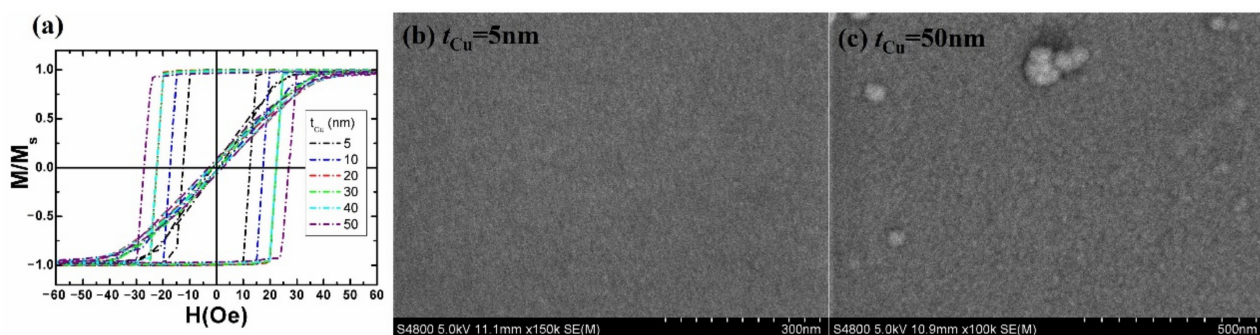


Figure 2. (a) The hysteresis loops along both easy axis and hard axis dependence on t_{Cu} . (b,c) are SEM photos of samples with thickness of 5 nm and 50 nm, respectively.

Figure 3 shows that the dependence of the easy-axis coercivity, hard-axis coercivity and saturation magnetization on the thickness of the Cu seed layer obtained from Figure 2a. It can be found that the easy-axis coercivity (H_{ce}) has an overall increasing trend with the thickness of Cu underlayer, which is similar to the results previously reported [7–9,16]. It is interesting that the easy-axis coercivity maintain a constant about 22.5 Oe for $20 \text{ nm} \leq t_{Cu} \leq 40 \text{ nm}$. Except for the slight decrease at $t_{Cu} = 30$ nm, the hard axis coercivity (H_{ch}) shows a slight increasing trend, which is similar to that observed in Ru/FeCo films. [16]. The value of saturation magnetization ($4\pi M_s$) shows a fluctuation around 7500 Gs as t_{Cu} increases. The deviation may be due to the volume measurement error of samples.

Figure 4 shows the complex permeability $\mu = \mu' - i\mu''$ versus frequency f at t_{Cu} increasing from 5 nm to 50 nm, where μ' and μ'' are the real and imaginary parts of the complex permeability, respectively. The open circles represent the experimental results which were obtained by micro-strip method and the solid line is the result calculated by fitting with Equation (2). For all the fittings, $4\pi M_s$ takes the value of 7.5 KGs from the measurements of VSM. The dependences of fitting parameters on t_{Cu} are shown in Figures 5 and 6.

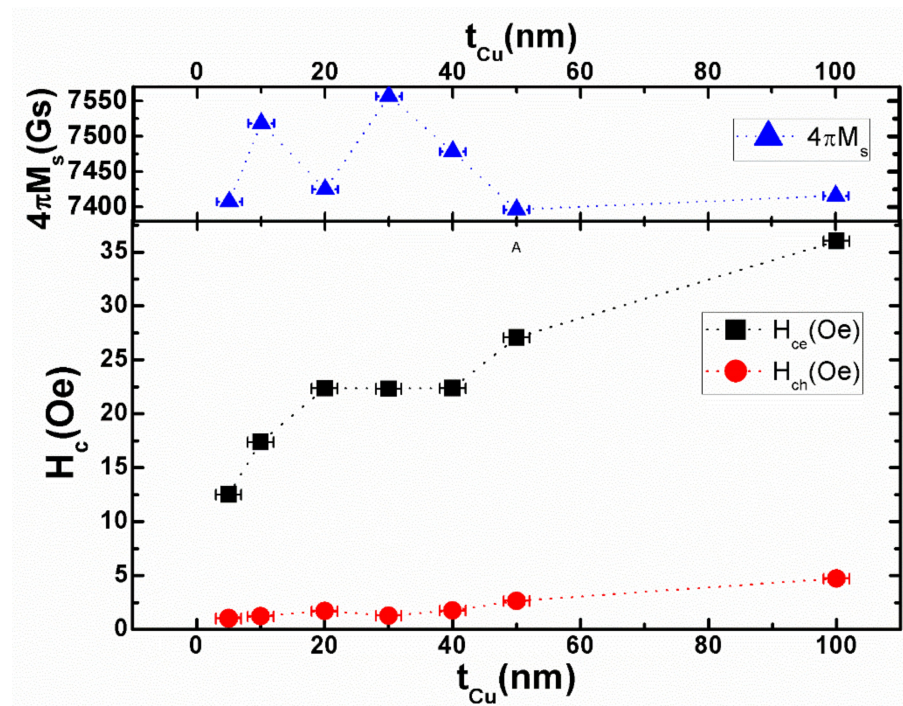


Figure 3. The t_{Cu} dependence of the saturation magnetization ($4\pi M_s$), the easy axis (H_{ce}) and hard axis (H_{ch}) coercivity for Cu/ $Ni_{80}Fe_{20}$ thin films.

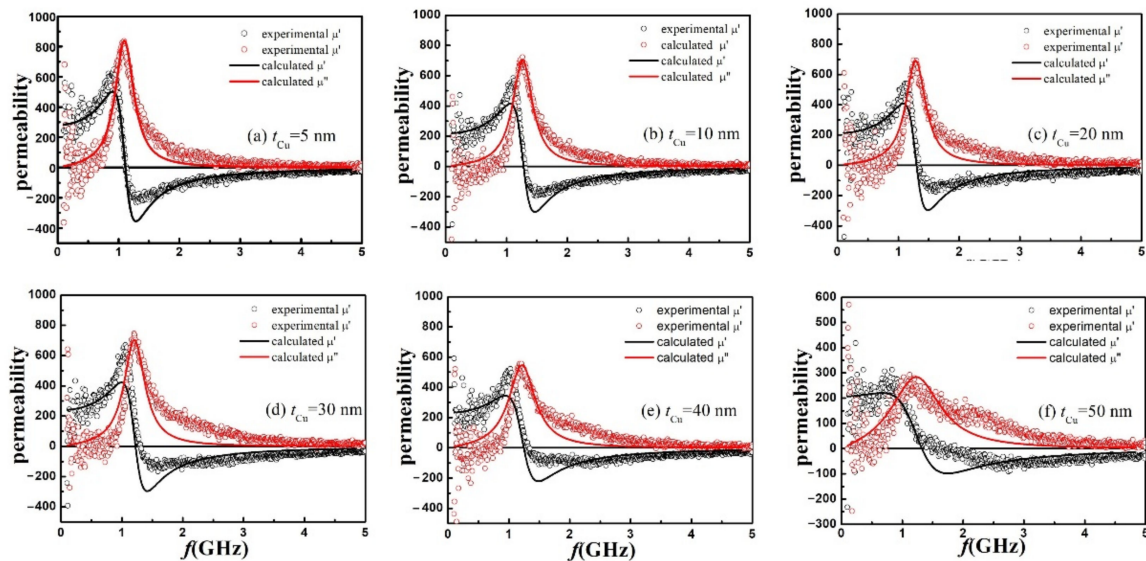


Figure 4. The permeability spectrum of the real μ' and imaginary μ'' components of the permeability of the samples with t_{Cu} increasing from 5 nm to 50 nm. The solid line is the fitting curve with the LLG model.

The static IPUMA field H_a can be calculated from the hysteresis loop by the following method. First the central line is approximated by the forward and backward branches of the sloping portion of the hard-axis hysteresis loop. The H_a is obtained by extrapolating the intersection of the slope of the centerline at the origin and the magnetization saturation line. While the dynamic IPUMA field H_k , namely, the effective IPUMA field, can be obtained by fitting the permeability spectrum by the LLG equation. Figure 5 shows the changes of H_a , H_k and $\Delta H_k (=H_a - H_k)$ with Cu thickness t_{Cu} . It is well known that the famous Hoffmann's ripple theory can be used to explain the decrease in H_k of soft magnetic thin films appropriately [17]. The ΔH_k value represents the strength of the ripple field induced

by Cu underlayer in the bilayer film [18], especially when the Cu underlayer thickness is 40 nm. The film's surface or interface roughness may be the reason that the magnetic ripple with an angular dispersion of anisotropy can be observed in the films [19,20]. For the formation mechanism of the IPUMA in our samples, we deduce that it can be interpreted from these two mechanisms. One mechanism is the thickness gradient caused by the obliquely sputtered Cu underlayer [20], and with the increase of thickness of Cu underlayer, the thickness gradient effect is stronger. Another mechanism is the shape anisotropy caused by the anisotropic surface undulation of the underlayer [6]. In our samples the IPUMA field is not monotonically increasing but has ups and downs with increasing t_{Cu} from Figure 5. Therefore, it can be inferred that the production of IPUMA in our samples is due to the combined effect of these two mechanisms. The inset of Figure 5 shows the resonance frequency f_r versus t_{Cu} . The change in H_k causes a change in the resonance frequency f_r , which is consistent with the formula $f_r = (\gamma/2\pi)\sqrt{M_s H_k}$ [5].

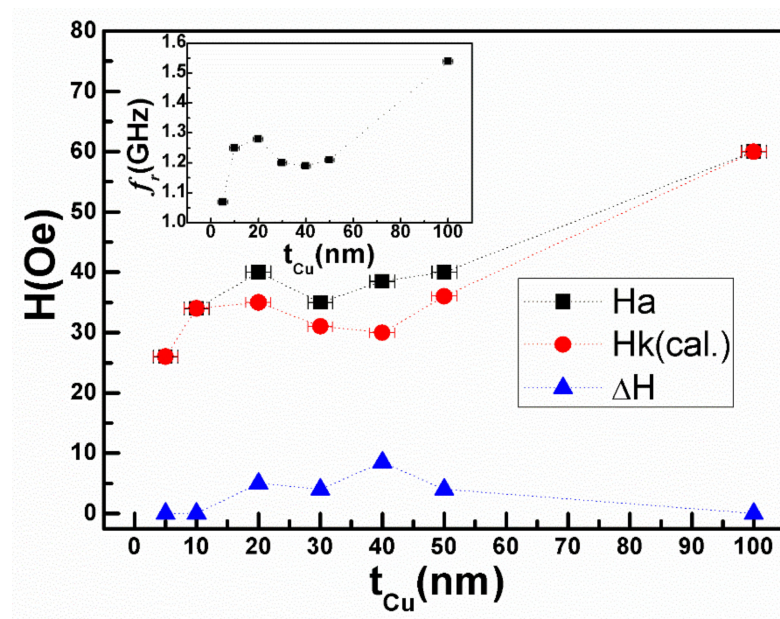


Figure 5. The IPUMA field H_a , the effective IPUMA field H_k and the difference $\Delta H_k (=H_a - H_k)$ versus Cu underlayer thickness t_{Cu} . The inset shows the resonance frequency f_r versus t_{Cu} .

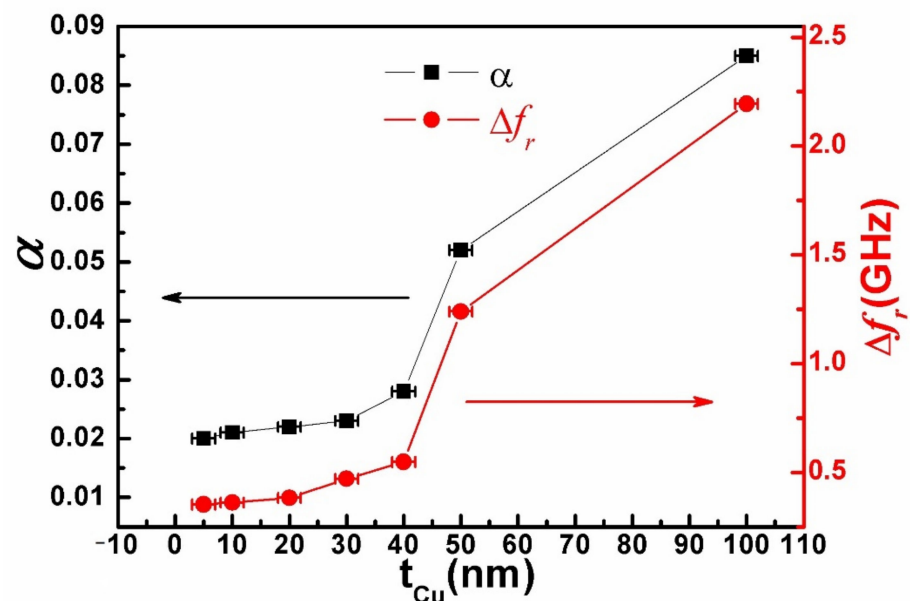


Figure 6. The dependence of α and Δf_r on Cu underlayer thickness t_{Cu} .

Figure 6 depicts the dependence of the resonance linewidth Δf_r and the damping factor α on t_{Cu} . Both Δf and α slowly increases for $t_{Cu} \leq 40$ nm, and then increases rapidly for $t_{Cu} \geq 40$ nm. According to the Equation (2), the resonance linewidth Δf is determined by α , since $\Delta f_r = \alpha(2f_0 + f_1) \approx \alpha f_1$ [2]. As expected, Δf shows the same tendency as α . Due to the stress relief of the film, Cu underlayer has a remarkable influence [21]. Generally, when the static soft magnetic performance is optimal, the damping factor α is the lowest, and a certain stress is beneficial to the optimization of soft magnetic properties [22]. This provides a conceivable explanation for the change of α . In our works, the large change of α can be mainly subject to the extrinsic damping. Extrinsic damping is mainly caused by the inhomogeneity [23] and the spin waves [24]. As the thickness of Cu underlayer becomes thicker, the spin-pumping effect will also lead to the enhancement of sample damping [25]. This is the possible reason for the damping factor increases sharply for $t_{Cu} \geq 40$ nm. We found that the damping factor α of the sample can be adjusted by controlling the thickness of the obliquely sputtered Cu underlayer.

4. Conclusions

In summary, an interesting method of the obliquely sputtered Cu underlayer for 50 nm Ni₈₀Fe₂₀ thin films was used to produce IPUMA and the magnetic properties of as-deposited Cu(t_{Cu} nm)/Ni₈₀Fe₂₀(50 nm) bilayer films dependent on t_{Cu} were investigated. The increasing tendency in H_{ce} and H_{ch} dependence of t_{Cu} are observed. The dynamic magnetic characteristic of all samples was analyzed based on the LLG equation. When the underlayer thickness is 40 nm, the largest ΔH_k which is from the magnetic ripple is obtained. The damping factor α proportional to Δf increases with the increasing thickness of the Cu underlayer. Our work provides a feasible method to adjust the damping factor of soft magnetic thin films in high-frequency applications.

Author Contributions: Conceptualization, X.L., Y.J. and T.L.; methodology, X.L.; software, M.C.; validation, X.L. and J.W.; formal analysis, X.L.; investigation, X.L. and Z.Z.; resources, L.Z.; data curation, X.L. and M.C.; writing—original draft preparation, X.L.; writing—review and editing, X.L. and Y.P.; visualization, X.L. and Y.P.; supervision, Y.J., T.L. and X.G.; project administration, G.P. and M.W.; funding acquisition, H.Y. All authors have read and agreed to the published version of the manuscript.

Funding: This work is supported by the National key research and development program of China (No. 2021YFF0700900), the national defense fundamental scientific research program for stable support project (No. SK2020-013, No. SK2021-023), and the key research and development project of Sichuan Science and Technology Plan program (No. 2021YFG0346).

Institutional Review Board Statement: Not applicable.

Informed Consent Statement: Not applicable.

Data Availability Statement: The data that support the findings of this study are available from the corresponding author, [Xiaoyu Li], upon reasonable request.

Acknowledgments: This work was supported by the Ninth Research Institute of China Electronics Technology Group Corporation and the University of Electronic Science and Technology of China.

Conflicts of Interest: The authors declare no conflict of interest.

References

1. Gilbert, T.L. A phenomenological theory of damping in ferromagnetic materials. *IEEE Trans. Magn.* **2004**, *40*, 3443. [[CrossRef](#)]
2. Xu, F.; Zhang, X.; Ma, Y.; Phuoc, N.N.; Chen, X.; Ong, C.K. Influence of Cu underlayer on the high-frequency magnetic characteristics of as-sputtered FeCoSiN granular thin films. *J. Phys. D Appl. Phys.* **2009**, *42*, 015002. [[CrossRef](#)]
3. Youssef, J.B.; Vukadinovic, N.; Billet, D.; Labrune, M. Thickness-dependent magnetic excitations in Permalloy films with nonuniform magnetization. *Phys. Rev. B* **2004**, *69*, 174402. [[CrossRef](#)]
4. Klemmer, T.J.; Ellis, K.A.; Chen, L.H.; van Dover, B.; Jin, S. Ultrahigh frequency permeability of sputtered Fe-Co-B thin films. *J. Appl. Phys.* **2000**, *87*, 830. [[CrossRef](#)]
5. Fan, X.; Xue, D.; Lin, M.; Zhang, Z.; Guo, D.; Jiang, C.; Wei, J. In situ fabrication of Co₉₀Nb₁₀ soft magnetic thin films with adjustable resonance frequency from 1.3 to 4.9 GHz. *Appl. Phys. Lett.* **2008**, *92*, 222505. [[CrossRef](#)]

6. McMichael, R.D.; Lee, C.G.; Bonevich, J.E.; Chen, P.J.; Miller, W.; Egelhoff, W.F., Jr. Strong anisotropy in thin magnetic films deposited on obliquely sputtered Ta underlayers. *J. Appl. Phys.* **2000**, *88*, 5296. [[CrossRef](#)]
7. Hadley, M.J.; Pollard, R.J. Magnetic and structural properties of Co films deposited onto obliquely sputtered Pt underlayers. *J. Appl. Phys.* **2002**, *92*, 7389. [[CrossRef](#)]
8. Zhao, Z.; Mani, P.; Mankey, G.J.; Gubbiotti, G.; Tacchi, S.; Spizzo, F.; Lee, W.-T.; Yu, C.T.; Pechan, M.J. Magnetic properties of uniaxial synthetic antiferromagnets for spin-valve applications. *Phys. Rev. B* **2005**, *71*, 104417. [[CrossRef](#)]
9. Umlor, M.T. Uniaxial magnetic anisotropy in cobalt films induced by oblique deposition of an ultrathin cobalt underlayer. *Appl. Phys. Lett.* **2005**, *87*, 082505. [[CrossRef](#)]
10. Fukuma, Y.; Lu, Z.; Fujiwara, H.; Mankey, G.J.; Butler, W.H.; Matsunuma, S. Strong uniaxial magnetic anisotropy in CoFe films on obliquely sputtered Ru underlayer. *J. Appl. Phys.* **2009**, *106*, 076101. [[CrossRef](#)]
11. McCord, J.; Kaltofen, R.; Schmidt, O.G.; Schultz, L. Tuning of magnetization dynamics by ultrathin antiferromagnetic layers. *Appl. Phys. Lett.* **2008**, *92*, 162506. [[CrossRef](#)]
12. Fassbender, J.; McCord, J. Control of saturation magnetization, anisotropy, and damping due to Ni implantation in thin Ni₈₁Fe₁₉ Layers. *Appl. Phys. Lett.* **2006**, *88*, 252501. [[CrossRef](#)]
13. Xu, F.; Phuoc, N.N.; Zhang, X.Y.; Ma, Y.G.; Chen, X.; Ong, C.K. Tuning of the magnetization dynamics in as-sputtered FeCoSiN thin films by various sputtering gas pressures. *J. Appl. Phys.* **2008**, *104*, 093903. [[CrossRef](#)]
14. Zhu, X.; Wang, Z.; Zhang, Y.; Xi, L.; Wang, J.; Liu, Q. Tunable resonance frequency of FeNi films by oblique sputtering. *J. Magn. Magn. Mater.* **2012**, *324*, 2899–2901. [[CrossRef](#)]
15. Bekker, V.; Seemann, K.; Leiste, H. A new strip line broad-band measurement evaluation for determining the complex permeability of thin ferromagnetic films. *J. Magn. Magn. Mater.* **2004**, *270*, 327. [[CrossRef](#)]
16. Lu, Z.; Fukuma, Y.; Butler, W.H.; Fujiwara, H.; Mankey, G.J.; Matsunuma, S. Magnetic Anisotropy of FeCo Films Induced by Obliquely Sputtered Ru Underlayers. *IEEE T. Magn.* **2009**, *45*, 40081010.
17. Hoffmann, H. Magnetic properties of thin ferromagnetic films in relation to their structure. *Thin Solid Film.* **1979**, *58*, 223. [[CrossRef](#)]
18. Lopusnik, R.; Nibarger, J.; Silva, T.; Celinski, Z. Different dynamic and static magnetic anisotropy in thin Permalloy films. *Appl. Phys. Lett.* **2003**, *83*, 96. [[CrossRef](#)]
19. Nguyen, L.T.; Lisfi, A.; Lodder, J.C. The effects of metallic underlayers on magnetic properties of obliquely sputtered Co thin films. *J. Magn. Magn. Mater.* **2002**, *374*, 242–245. [[CrossRef](#)]
20. Lisfi, A.; Lodder, J.C.; Wormeester, H.; Poelsema, B. Reorientation of magnetic anisotropy in obliquely sputtered metallic thin films. *Phys. Rev. B* **2002**, *66*, 174420. [[CrossRef](#)]
21. Jung, H.S.; Doyle, W.D.; Wittig, J.E.; Al-Sharab, J.F.; Bentley, J. Influence of underlayers on the soft properties of high magnetization FeCo films. *Appl. Phys. Lett.* **2002**, *81*, 2415. [[CrossRef](#)]
22. Zou, P.; Winnie, Y.; Bain, J.A. Influence of stress and texture on soft magnetic properties of thin films. *IEEE Trans. Magn.* **2002**, *38*, 3501.
23. Bonin, R.; Schneider, M.L.; Silva, T.J.; Nibarger, J.P. Dependence of magnetization dynamics on magnetostriction in NiFe alloys. *J. Appl. Phys.* **2005**, *98*, 123904. [[CrossRef](#)]
24. Counil, G.; Kim, J.; Devolder, T.; Chappert, C.; Shigeto, K.; Otani, Y.J. Spin wave contributions to the high-frequency magnetic response of thin films obtained with inductive methods. *Appl. Phys.* **2004**, *95*, 5646. [[CrossRef](#)]
25. Tserkonvyak, Y.; Brataas, A.; Bauer, G.E.W. Enhanced Gilbert Damping in Thin Ferromagnetic Films. *Phys. Rev. Lett.* **2002**, *88*, 117601. [[CrossRef](#)]